Preprints of the 21st IFAC World Congress (Virtual)
Berlin, Germany, July 12-17, 2020

Adaptive Variable Synthetic Inertia from a Virtual Synchronous Machine Providing Ancillary Services for an AC MicroGrid

Filipe Perez [*,**] **Gilney Damm** [*]
Françoise Lamnabhi-Lagarrigue [*] **Paulo Ribeiro** [**]
Renato Monaro [***]

[*] *L2S Laboratory, CNRS-CentraleSupélec, Paris-Saclay University, 3 rue Joliot-Curie, 91192, France (filipe.perez@centralesupelec.fr)*
[**] *ISEE Institute, Federal University of Itajubá, Avenida BPS 1303, 37500 903, Itajubá, Brazil (pfribeiro@ieee.org)*
[***] *Polytechnic School, University of São Paulo, Av. Prof. Luciano Gualberto 380, 05508 010, São Paulo, Brazil (monaro@usp.br)*

Abstract: The paper proposes an adaptive variable synthetic inertia strategy to provide frequency and voltage support (ancillary services) in an AC MicroGrid (weak grid) composed of diesel generators and loads. A DC MicroGrid is connected to the AC one by a Voltage Source Converter (VSC). The VSC converter is driven as a Virtual Synchronous Machine (VSM), where the control strategy follows a swing equation such the converter emulates a synchronous machine, including inertial support. A rigorous stability analysis is developed based on Lyapunov technique assuring proper stability conditions for an adaptive inertia designated, such that, frequency stability is improved and power oscillations are reduced. This strategy can be exploited in low inertia systems like MicroGrids or grids with high penetration of renewables. Simulation results illustrate the performance of the proposed control and the system's operation, where a comparison with droop control is presented.

Keywords: Ancillary Services, Frequency and Voltage Support, Virtual Inertia, Lyapunov Technique, AC/DC MicroGrid, Low Inertia Grids.

1. INTRODUCTION

Electric power networks are currently going through a large transformation. Historically, they were based on synchronous machines rotating in synchronism, with the grid frequency, and providing natural inertia in response to disturbances or simply changes on operating conditions. This classical scheme is less and less true, because of the large penetration of power electronic devices, the power converters. These are inherent to the interconnection of renewable energy sources and storage units, but also by the High Voltage Direct Current (HVDC) lines that are being built to reinforce current transmission systems. For this reason inertia is reducing fast, and in some situations grids can be mostly composed of power converters (Tielens and Van Hertem, 2016; Winter et al., 2014; Milano et al., 2018). This situation is a change of paradigm from the classic electric grid, and power systems practitioners are struggling to keep the grid running. A recent example of such situation is the 9 august 2019 black-out in the United Kingdom (National grid ESO , 2019) where the main cause was the reduction of inertia, and its effect in several power converters interconnecting distributed generation.

An interesting possibility for solving these problems, is represented by the concept of synchronverters (Zhong and Weiss, 2010). These are composed by power converters that mimic synchronous machines, called in the paper Virtual Synchronous Machine (VSM) [1]. In this way, it is much easier to integrate such systems to the power network, providing a framework that practitioners are well acquainted (D'Arco et al., 2015b; Tamrakar et al., 2017). These synchronverters have raised much interest in recent years, illustrated by the keynote talk *Synchronized and Democratized Smart Grids to Underpin the Third Industrial Revolution* from Qing-Chang Zhong on the *IFAC World Congress 2017*.

Many studies have been carried out concerning the application of virtual inertia in power converters, such as integration of distribution generation (D'Arco et al., 2015b), improvements in MicroGrids (Shi et al., 2018) and isolated power systems (D'Arco et al., 2015a). In (Liu et al., 2015), a comparison on the dynamics between virtual inertia and droop control strategy is done, pointing out the similarities and the advantages of each control strategy, as well as the relevance of inertia properties. As the next step, new propositions on virtual inertia emerged, for example, in (Alipoor et al., 2014), the parameters of VSM can be controlled, and then, VSM with alternating moment of inertia is developed. The damping effect of the alternating inertia scheme is investigated by transient energy analysis. In (Hou et al., 2019), an adaptive virtual inertia is proposed

[1] Note that VSM is said as the Voltage Source Converter operating as a synchronous machine.

to improve dynamic frequency regulation of MicroGrid, where the control strategy match the advantages of large inertia and small inertia properties during transients.

The present work is dedicated to these systems, but now acknowledging that if they act as synchronous machine, they are not limited to this behaviour, and can provide extended support than a physical machine does. In this way, it was studied the contribution that Virtual Synchronous Machines may bring to the overall inertia of a power grid, and how they can provide ancillary services, in particular frequency support and synthetic inertia. This approach, in large part inspired by adaptive control, assures through a Lyapunov function, asymptotic stability of the overall system. Simulation results illustrate the great contribution such Variable Synthetic Inertia can bring to a low inertia system. In particular, this approach can contribute to solve the problems brought by renewable sources in modern power systems, and allow much larger penetration of such intermittent energies.

2. ELECTRICAL MODEL

The electrical model in this work has been addressed in two parts: The MicroGrid and the virtual synchronous machine model.

2.1 MicroGrid model

The paper proposes a Virtual Synchronous Machine (VSM) using an adaptive virtual inertia approach to improve frequency stability and reduce power oscillations in the grid. The variable inertia scheme is incorporated in a VSC converter connected to an AC MicroGrid composed by a diesel generator and loads. The DC side of the grid is formed by a DC MicroGrid able to provide energy (ancillary services) to the AC side of the grid. The DC part will be not detailed here (see (Perez et al., 2019)), being summarized as a voltage V_{DC} where its dynamics are not considered. In Fig. 1 is presented the electrical model of the system.

The VSC converter has a LC filter, represented by L_c and C_c, connected to the Point of Common Coupling (PCC) with the AC MicroGrid. The line impedance is represented by L_l and the active losses are given by R_l. The state space model of the system can be written as:

$$\dot{I}_{c,d} = -\frac{R_c}{L_c} I_{c,d} + \omega_g I_{c,q} + \frac{1}{2L_c} V_{DC} m_d - \frac{V_{c,d}}{L_c} \quad (1)$$

$$\dot{I}_{c,q} = -\frac{R_c}{L_c} I_{c,q} - \omega_g I_{c,d} + \frac{1}{2L_c} V_{DC} m_q - \frac{V_{c,q}}{L_c} \quad (2)$$

$$\dot{V}_{c,d} = \frac{I_{c,d}}{C_c} - \frac{I_{l,d}}{C_c} + \omega_g V_{c,q} \quad (3)$$

$$\dot{V}_{c,q} = \frac{I_{c,q}}{C_c} - \frac{I_{l,q}}{C_c} - \omega_g V_{c,d} \quad (4)$$

$$\dot{I}_{l,d} = -\frac{R_l}{L_l} I_{l,d} + \omega_g I_{l,q} + \frac{V_{c,d}}{L_l} - \frac{V_{l,d}}{L_l} \quad (5)$$

$$\dot{I}_{l,q} = -\frac{R_l}{L_l} I_{l,q} - \omega_g I_{l,d} + \frac{V_{c,q}}{L_l} - \frac{V_{l,q}}{L_l} \quad (6)$$

From Park transformation we have: $V_{c,(dq)}$ the voltage on the LC filter capacitor C_c, $I_{c,(dq)}$ the current on the

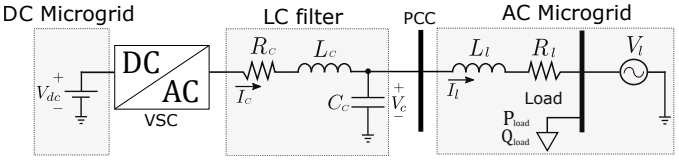

Fig. 1. Virtual Synchronous Machine connected to a AC MicroGrid based on diesel generation.

LC filter inductor L_c. $I_{l,(dq)}$ the line current, V_l is the voltage on the diesel generator, and P_{load} and Q_{load} are the active and reactive power of the load in the AC MicroGrid respectively. The angular speed is given by ω_g, where $\omega_g = 2\pi f_g$. The DC/AC converter modulation indexes are m_d and m_q.

2.2 Virtual synchronous machine model

A VSM can act to provide transient power sharing and primary control frequency support independently, using only local measurements. VSM can also be implemented with no need of Phase-locked Loop (PLL), being used just for sensing the grid frequency or during initial machine starting [2]. As result, VSM are conceptually simple thanks to intuitive interpretation as synchronous machines responses (D'Arco et al., 2015a; Tamrakar et al., 2017).

To develop a VSM it is necessary to implement the swing equation of a Synchronous Machine in the VSC control structure as detailed in (Zhong and Weiss, 2010). In the following, is presented a general swing equation of a synchronous machine applied for VSM implementation, where the inertia acceleration is represented by the power balance and a damping factor:

$$\dot{\tilde{\omega}} = \frac{1}{H}[P_{ref} - P - D_p(\omega_{vsm} - \omega_g)] \quad (7)$$

with $\tilde{\omega} = \omega_{vsm} - \omega_g$ being the frequency deviation, ω_{vsm} the VSM's frequency, H the virtual inertia coefficient and D_p the damping factor. P_{ref} is the active power droop reference and P is the measured power into the AC grid.

The inertia coefficient is defined in (Kundur et al., 1994):

$$H = \frac{S_{nom}}{2J\omega_o^2} \quad (8)$$

where S_{nom} is the nominal apparent power of the VSC converter, ω_o is nominal grid value and J is the emulated moment of inertia. In (8), it is evident the inverse ratio between moment of inertia and its time constant. H unit is given is seconds, therefore, the larger the inertia coefficient becomes, the lower the frequency deviation and the longer accommodation time, and vice-versa, the smaller the inertia coefficient becomes, the higher the frequency deviation and the shorter accommodation time. This idea is going to be used for variable inertia formulation.

3. PROPOSED CONTROL STRATEGY

This section provides the control strategy to implement the virtual synchronous machine on the MicroGrid's VSC

[2] The swing equation of VSM allows interactions with the grid frequency, influencing its behavior.

and the application of variable virtual inertia to provide ancillary services.

The power reference is calculated by an active power-frequency droop strategy, included in the swing equation (7), relating active power with angular speed deviation as follows:

$$P_{ref} = P^* - K_\omega[\omega_{vsm} - \omega^*] \tag{9}$$

where P^* is the desired active power to be injected/ absorbed into the grid. K_ω is the $P-f$ droop gain and ω^* is the angular speed reference, i.e. $\omega^* = \omega_o$. In this case, the angular speed ω_{vsm} computed in (7) can be integrated to obtain VSM phase angle $\delta_{vsm} = \int \omega_{vsm} dt$.

Voltage reference is also calculated by a reactive power-voltage droop strategy, where the voltage is controlled at the PCC (LC filter voltage on capacitor C_c). From synchronous reference frame, voltage $V_{c,d}$ reefers to the voltage module, and then to regulate the voltage amplitude, the following droop equation is presented:

$$V_{c,d_{ref}} = V^*_{c,d} - K_q[Q - Q^*] \tag{10}$$

$V^*_{c,d}$ is the desired voltage amplitude and Q^* is the desired reactive power injected/absorbed into the grid, with K_q being the droop gain for reactive power. The converter voltage $V_{c,d}$ is controlled to reach $V_{c,d_{ref}}$ using a PI controller, and the PLL is used to measure the frequency of the grid ω_g, therefore we can consider $V_{c,q} = 0$.

Equations (9) and (10) are known as the droop reference for respectively the Active Power and Voltage, and represent primary ancillary services. They are seen as a higher level control for the overall power grid.

According to control target, frequency (ω_{vsm}) and voltage ($V_{c,d}$) are chosen as the control output. Modulation indexes (m_d and m_q) provide the reference to generate the PWM signals, where m_d and m_q is transformed into phasor signal with amplitude m and phase θ, chosen as the control inputs. The phase angle is given by δ_{vsm} from the swing equation in (7) and voltage reference $V_{c,d_{ref}}$ is given by the droop strategy in (10):

$$\frac{1}{2} m V_{dc} \angle\theta = V_{c,d_{ref}} \angle\delta_{vsm} \tag{11}$$

The signal obtained in (11) is the reference signal for the PMW modulation, making possible to emulate inertia in the VSC converter (Zhong and Weiss, 2010).

3.1 Variable inertia formulation

To propose the inertia variation, we rewrite the swing equation of a synchronous machine, noting that $\dot{\delta} = \omega_{vsm} - \omega_g$. Equation (7) is rewritten as follows:

$$H\ddot{\delta} = P_{ref} - P_{max} sin(\delta) - D_p\dot{\delta} \tag{12}$$

where $\delta = \delta_{vsm} - \delta_g$ is the power angle difference between the diesel generator and the VSC, $P_{max} sin(\delta)$ is the maximum available power [3] . Defining $\tilde{\omega} = \omega_{vsm} - \omega_g$, then, multiplying last equation by $\tilde{\omega}$, we may obtain:

[3] The maximum available power is the nominal power of the VSC or the diesel generator, depending on the power angle δ.

$$H\tilde{\omega}\dot{\tilde{\omega}} - P_{ref}\tilde{\omega} + P_{max}\tilde{\omega} sin\delta + D_p\tilde{\omega}^2 = 0 \tag{13}$$

The energy of the system from a equilibrium point ($\delta = \bar{\delta}; \tilde{\bar{\omega}} = 0$) can be calculated by integrating equation above as:

$$H\int_0^{\tilde{\omega}} \tilde{\omega} d\omega - P_{ref}\int_{\bar{\delta}}^{\delta} d\delta + P_{max}\int_{\bar{\delta}}^{\delta} sin(\delta) d\delta = C \tag{14}$$

with C being a constant of integration. The dissipated energy (damping term) is not considered, obtaining then this well known Lyapunov candidate in (15), considering just potential (E_p) and kinetic (E_k) energy introduced in (Machowski et al., 2011).

$$V = \frac{1}{2} H\tilde{\omega}^2 - P_{ref}(\delta - \bar{\delta}) - P_{max}(cos\delta - cos\bar{\delta}) \tag{15}$$

The time-derivative of the Lyapunov candidate following the energy function (Kundur et al., 1994):

$$\dot{V} = \frac{\partial E_k}{\partial\tilde{\omega}}\frac{d\tilde{\omega}}{dt} + \frac{\partial E_p}{\partial\delta}\frac{d\delta}{dt} \tag{16}$$

Therefore, considering the inertia coefficient H as time varying, the time-derivative of the Lyapunov candidate can be computed as:

$$\dot{V} = \frac{1}{2}\tilde{\omega}^2\frac{dH}{dt} + H\tilde{\omega}\dot{\tilde{\omega}} - P_{ref}\dot{\delta} + P_{max} sin(\delta)\dot{\delta} \tag{17}$$

We can now state a time varying variable for the inertia coefficient, such that, stability can be proved. The proposed variable inertia coefficient is written as:

$$\begin{aligned} H &\approx H_o + K_M\tilde{\omega}\dot{\tilde{\omega}} \\ H &\triangleq H_o + K_M\tilde{\omega}\frac{1}{H_0}[P_{ref} - P_{max} sin(\delta) - D_p\tilde{\omega}] \end{aligned} \tag{18}$$

where H_o is a constant inertia coefficient, kept in steady-state and K_M is interpreted as a positive gain. The inertia coefficient is saturated such as to have $H_{min} \leq H \leq H_{max}$ for suitable constants H_{min} and H_{max} to assure the desired behavior of the electric grid. The angular speed deviation ($\tilde{\omega}$) and its derivative ($\dot{\tilde{\omega}}$) play a important role to change significantly the inertia value during transients. The variable inertia coefficient proposed in (18) is replaced in the swing equation in (7). Therefore, a improved inertial support can be implemented in the VSC converter of the MicroGrid (Hou et al., 2019).

To explain the action of the proposed variable inertia coefficient, we may summarize:

(1) When $\tilde{\omega} > 0$ and $\dot{\tilde{\omega}} > 0$ or $\tilde{\omega} < 0$ and $\dot{\tilde{\omega}} < 0$, the machine is in accelerating process, which means that angular speed is deviating from its original value. Therefore, the inertia should increase to minimize frequency deviation (inertial support).
(2) When $\tilde{\omega} < 0$ and $\dot{\tilde{\omega}} > 0$ or $\tilde{\omega} > 0$ and $\dot{\tilde{\omega}} < 0$, the machine is in decelerating process, which means that angular speed is returning to its steady-state value. Therefore, the inertia should decrease to allow fast return to new equilibrium point.

In this way, it is possible to damp frequency and power oscillation more efficiently than keeping constant inertia.

3.2 Stability analysis

The time-derivative of the proposed Lyapunov function in (15) is finally obtained working on equation (17):

$$\dot{V} = \frac{1}{2}\dot{H}\tilde{\omega}^2 - D_p\tilde{\omega}^2 \tag{19}$$

So, taking the inertia definition (18), it's derivative is:

$$H = H_o + K_M\tilde{\omega}\frac{1}{H_0}(P_{ref} - P_{max}sin(\delta) - D_p\tilde{\omega})$$
$$\dot{H} = \frac{K_M}{HH_0}(P_{ref} - P_{max}sin(\delta) - D_p\tilde{\omega})^2 +$$
$$-\frac{K_M}{H_0}P_{max}cos(\delta)\tilde{\omega}^2 + \frac{K_M D_p^2}{HH_0}\tilde{\omega}^2 +$$
$$-\frac{K_M D_p}{HH_0}\tilde{\omega}(P_{ref} - P_{max}sin(\delta))$$

It is easy to see that inside a given operation region $\|\tilde{\omega}\| \leq \tilde{\omega}_{max}$, $\|(\delta - \bar{\delta})\| \leq \tilde{\delta}_{max}$, for K_M properly chosen such that dH/dt is smaller than $2D_p$, one obtains a negative semi-definite function ($\tilde{\omega}_{max}$, $\tilde{\delta}_{max}$ and C_1 suitable constants):

$$\dot{V} = -C_1\tilde{\omega}^2 \tag{20}$$

Indeed, for K_M smaller than a limit value: $dH/dt < 2D_p + C_1$, where K_M can be of several thousands of unities for typical values. Equation (20) together with (15) assure boundedness of all states. From this, calling upon La Salle's theorem, we may now conclude that the system is asymptotically stable toward its equilibrium point.

4. SIMULATION RESULTS

The proposed model was built on *Matlab/Simulink* using *SimPowerSystems* toolbox. The converter that interfaces a DC MicroGrid (not presented in this paper) is connected to an AC one composed of a diesel generator and loads as depicted in Fig. 1. The diesel generator in the AC MicroGrid have a Governor [4] (speed control) to control the frequency and active power and an AVR [5] (Automatic Voltage Regulator) to control voltage and reactive power. The virtual synchronous machine and the AC grid parameters are presented in Table 1. The nominal frequency of the grid is $f_n = 50Hz$ and the nominal power of the diesel generator is $S_{diesel} = 2MVA$ with $V_l = 400V$ rms nominal voltage, 2 pairs of poles and inertia coefficient of $H_{diesel} = 3s$. The $Q - V$ droop coefficient is $K_q = 0.3$.

Table 1. MicroGrid parameters

VSC	$S_{nom} = 1MVA$	$f_s = 20kHz$	$\hat{V}_{c,nom} = 400V$
LC Filter	$R_c = 20m\Omega$	$L_c = 0.25mH$	$C_c = 150\mu F$
VSM	$K_w = 20$	$D_p = 50$	$H_o = 2s$
AC grid	$R_l = 0.1\Omega$	$L_l = 0.01mH$	$V_{l,nom} = 400V$

Here, the virtual synchronous machine have a nominal power of $S_{vsm} = 1MVA$ and same nominal rms voltage on the grid $V_{vsm} = 400V$, where this values are the base for per unit transformation. The load profile is depicted in Fig. 2, where the active and reactive power variation is shown. Large load variations were considered in simulations, up to 50% of the total load, to analyze the virtual inertia response under large disturbances. The maximum power consumption is $P_{max} = 2.3MW$ and $Q_{max} = 0.25MVAr$.

[4] Regulator gain $K = 150$ and time constant $T_{reg} = 0.1s$; actuator time constant $T_{act} = 0.25s$ and engine time delay $T_d = 0.024s$.
[5] Voltage regulator gain $K_{va} = 400$, time constant $T_{va} = 0.02s$ and low pass filter time constant $T_r = 0.02s$.

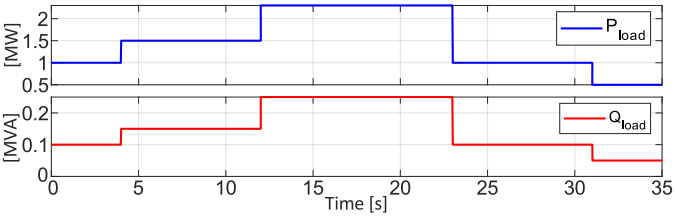

Fig. 2. AC load profile in the MicroGrid.

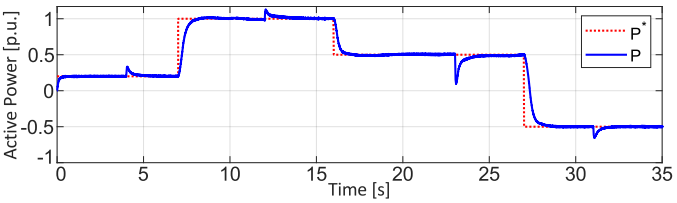

Fig. 3. The active power P from VSM into the AC grid and its desired power dispatch P^*.

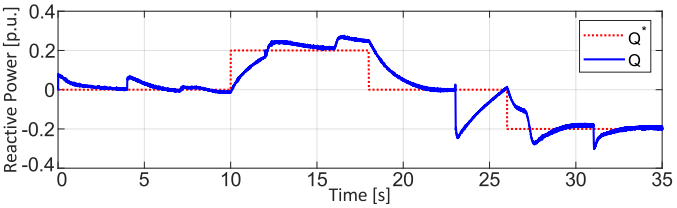

Fig. 4. The reactive power Q from VSM into the AC grid and its desired power dispatch Q^*.

The virtual synchronous machine is controlled to dispatch active power to assist the diesel generator on the power supply. Fig. 3 presents desired power P^* to be injected into the MicroGrid by the VSM and measured active power P. In Fig. 4 is presented the reactive power injected into the grid according to the desired voltage and reactive power profile. The control of voltage and reactive power is made by the droop control presented in (10). The reactive power behavior does not go exactly to the desired reactive power profile (Q^*), since the voltage have to be also controlled in the desired level (V_c^*). Then, reactive power supply changes to attain the voltage in the desired level as depicted in Fig 5.

The voltage profile on point of common coupling (after LC filter) is depicted in Fig. 5. The voltage is well controlled by the droop control in the desired value, even with some transient and steady-state deviations. They are because of the coupling between active power and voltage, since in this MicroGrid we have low X/L relation, which means that the grid is resistive (usual in isolated systems).

Once the active power was properly regulated by the VSM as shown in Fig. 3, the frequency of the grid should be controlled, such that system stability is attained. It means balance the injected power by the generator with the load demanded power. But, in this case, we have a low

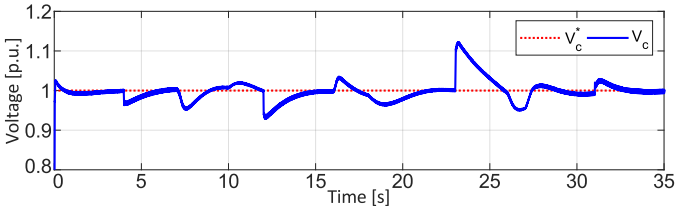

Fig. 5. V_c voltage profile on the PCC.

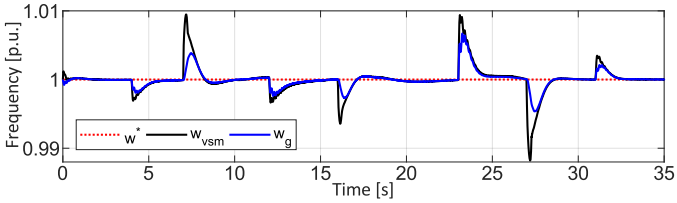

Fig. 6. Grid frequency ω_g with the angular speed on the VSM (ω_{vsm}) and frequency reference ω^*.

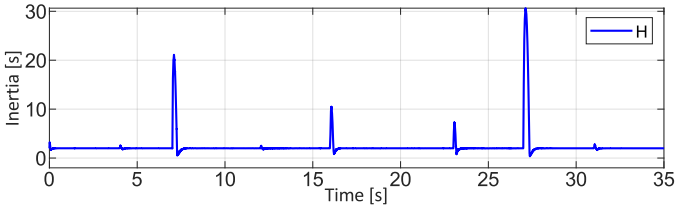

Fig. 7. Inertia coefficient behavior varying during frequency transients.

inertia system represented by the diesel generator, where the stability can be compromised by a large load change. Therefore, the VSM is used to assure frequency stability in the AC MicroGrid, by using a virtual inertia. Moreover, a variable inertia is proposed here to improve frequency stability and provide inertial support.

Fig. 6 depicts the behavior of the grid frequency ω_g, with the angular speed ω_{vsm} produced by the VSM and the angular speed reference ($\omega^* = 1\ p.u.$). The transient variations outcome from load variations (in 4, 12, 23 and 31 seconds of simulation time) and active power reference changes (in 7, 16 and 27 seconds). As expected, the bigger the power change, the larger the frequency excursion.

The variable inertia calculated in (18), is then applied in the VSM control law. Again, the main idea is to have an inertia coefficient H that varies according to frequency deviation $\tilde{\omega}$ and angular acceleration $\dot{\tilde{\omega}}$. Therefore, when VSM is accelerating, the inertia increases to minimize frequency deviation and when VSM is decelerating, the inertia decreases to speed-up reaching steady-state. The behavior of the variable inertia coefficient can be seen in Fig. 7. The transient behavior of the inertia is a consequence of $\dot{\tilde{\omega}}$ and $\tilde{\omega}$ as shown in Fig. 8, where the zoom presents the largest transients in these variables.

4.1 Comparison with droop control

To perform a complete analysis of the proposed control strategy, a comparison with well know techniques is required. Droop control strategy is widely used in Micro-Grids to share load demand among generators to balance the power and to assure frequency and voltage stability.

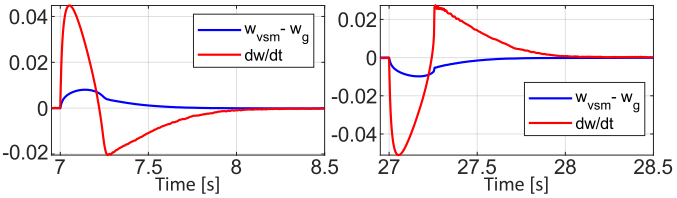

Fig. 8. Zoom in frequency deviation $\tilde{\omega}$ and in angular acceleration $\dot{\tilde{\omega}}$ during the largest transients.

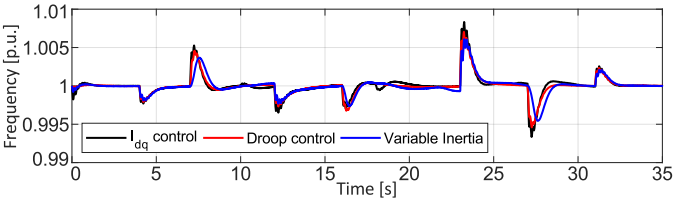

Fig. 9. Frequency of the grid considering different control approaches.

Therefore, a comparison between virtual inertia strategy and droop control is developed here.

The droop control is developed as follows:

$$P_{droop} = P^* - K_p(\omega_g - \omega^*) \tag{21}$$

where P_{droop} is the resultant power reference in this strategy and K_p is the droop coefficient that relates active power with frequency variation. The coefficient is chosen as $K_p = 5$ according to the limits of power and frequency.

To realize the comparison, the traditional $I_{d,q}$ control is also developed, where these currents are controlled, such that, active and reactive power is controlled in the desired value (P^* and Q^*). In this case, the only control target is to reach references, given by the following relation:

$$I^*_{c,d} = \frac{P^*}{V_{cd}}\ ; \quad I^*_{c,q} = \frac{Q^*}{V_{cd}} \tag{22}$$

Fig. 9 introduces the behavior of the frequency for each control strategy. The frequency response for standard $I_{d,q}$ control is considered the worse case, since it have highest overshoots and more oscillations. The variable inertia presents best transient response, which improve frequency stability and provide inertial support. The droop control presents a worse frequency behavior compared with virtual inertia strategy, since the transient variations are larger and more oscillatory than virtual inertia approach. Also, the droop control is not able to perform inertial support, which may result in instability problems.

A zoom in the largest transient of frequency is depicted in Fig. 10, where is clearly seen that droop control and $I_{d,q}$ control present almost the same behavior with no inertial support while the virtual inertia approach reduces the frequency deviation during load changes and power perturbations, improving frequency Nadir and RoCoF.

4.2 Comparison between different inertia coefficients

In this subsection, a comparison between constant inertia coefficient and a variable one is made. The idea is to compare how the frequency deviation changes when the inertia is fixed and how is the response for changing the coefficient K_M in the variable inertia approach. Four

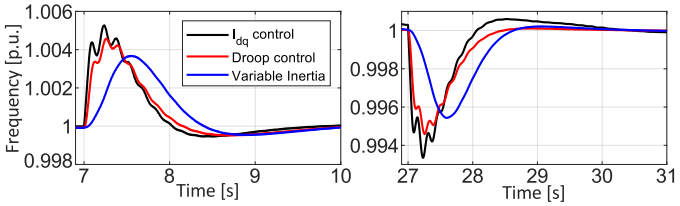

Fig. 10. Zoom in the frequency to compare the control strategies.

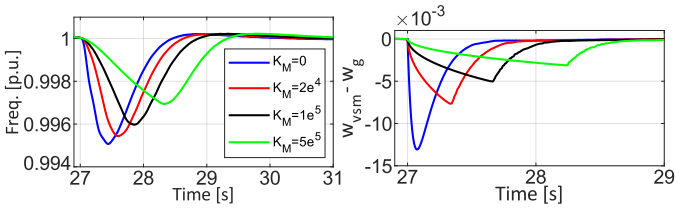

Fig. 11. Grid frequency on left and frequency deviation on right for different variation in the inertia coefficients.

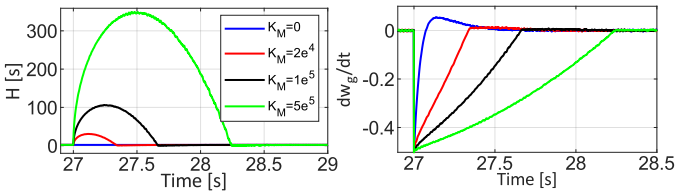

Fig. 12. Inertia coefficient on left and angular acceleration on right over different values of K_M.

different scenarios are simulated, first with constant inertia (which means $K_M = 0$), second $K_M = 2e^4$, third $K_M = 1e^5$ and fourth $K_M = 5e^5$, where for the proposed values of K_M, equation (20) is always valid.

As coefficient K_M increases, the frequency deviation decreases, improving the transient frequency response in the MicroGrid. This can be clearly shown in Fig. 11, where the four scenarios are presented with a zoom. Fig. 12 presents how the moment of inertia changes according to the coefficient K_M, making possible larger inertia coefficients to reduce frequency deviations (improve frequency Nadir and RoCoF). Also is presented how the angular acceleration behaves in these cases. All of these figures are zoomed in to depict the largest transient during simulations.

5. CONCLUSIONS

This paper proposes a variable virtual inertia scheme applied to a VSC converter to improve frequency stability and reduce power oscillations in a low inertia MicroGrids. The AC MicroGrid is composed by a diesel generator and loads, plus a VSC converter interfacing it to a DC MicroGrid. The proposed scheme is analyzed through a Lyapunov function that assures asymptotic stability for the system under the proposed variable inertia.

Simulation results shows that VSM helps the system providing frequency regulation and inertial support. This approach is compared to similar ones, and it is shown its improvement compared to classical droop control, since that one presents no inertia support. Therefore, we can conclude that variable inertia virtual synchronous machine is a good strategy to provide ancillary services for low inertia systems like MicroGrids.

REFERENCES

Jaber Alipoor, Yushi Miura, and Toshifumi Ise. Power system stabilization using virtual synchronous generator with alternating moment of inertia. *IEEE Journal of Emerging and Selected Topics in Power Electronics*, 3 (2), 2014.

Salvatore D'Arco, Jon Are Suul, and Olav B Fosso. Small-signal modeling and parametric sensitivity of a virtual synchronous machine in islanded operation. *International Journal of Electrical Power & Energy Systems*, 72:3–15, 2015a.

Salvatore D'Arco, Jon Are Suul, and Olav B Fosso. A virtual synchronous machine implementation for distributed control of power converters in smartgrids. *Electric Power Systems Research*, 122:180–197, 2015b.

Xiaochao Hou, Yao Sun, Xin Zhang, Jinghang Lu, Peng Wang, and Josep M Guerrero. Improvement of frequency regulation in vsg-based ac microgrid via adaptive virtual inertia. *IEEE Transactions on Power Electronics*, 35(2), 2019.

Prabha Kundur, Neal J Balu, and Mark G Lauby. *Power system stability and control*, volume 7. McGraw-hill New York, 1994.

Jia Liu, Yushi Miura, and Toshifumi Ise. Comparison of dynamic characteristics between virtual synchronous generator and droop control in inverter-based distributed generators. *IEEE Transactions on Power Electronics*, 31(5), 2015.

Jan Machowski, Janusz Bialek, and Jim Bumby. *Power system dynamics: stability and control*. John Wiley & Sons, 2011.

Federico Milano, Florian Dörfler, Gabriela Hug, David J Hill, and Gregor Verbič. Foundations and challenges of low-inertia systems. In *2018 Power Systems Computation Conference (PSCC)*. IEEE, 2018.

National grid ESO . Interim report into the low frequency demand disconnection (lfdd) following generator trips and frequency excursion on 9 aug 2019. 2019.

Filipe Perez, Alessio Iovine, Gilney Damm, Lilia Galai-Dol, and Paulo F Ribeiro. Stability analysis of a dc microgrid for a smart railway station integrating renewable sources. *IEEE Transactions on Control Systems Technology*, 2019.

Kai Shi, Haihan Ye, Wentao Song, and Guanglei Zhou. Virtual inertia control strategy in microgrid based on virtual synchronous generator technology. *IEEE Access*, 6, 2018.

Ujjwol Tamrakar, Dipesh Shrestha, Manisha Maharjan, Bishnu P Bhattarai, Timothy M Hansen, and Reinaldo Tonkoski. Virtual inertia: Current trends and future directions. *Applied Sciences*, 7(7), 2017.

Pieter Tielens and Dirk Van Hertem. The relevance of inertia in power systems. *Renewable and Sustainable Energy Reviews*, 55, 2016.

Wilhelm Winter, Katherine Elkington, Gabriel Bareux, and Jan Kostevc. Pushing the limits: Europe's new grid: Innovative tools to combat transmission bottlenecks and reduced inertia. *IEEE Power and Energy Magazine*, 13 (1), 2014.

Qing-Chang Zhong and George Weiss. Synchronverters: Inverters that mimic synchronous generators. *IEEE Transactions on Industrial Electronics*, 58(4), 2010.